



# Cellulose triacetate films obtained from sugarcane bagasse: Evaluation as coating and mucoadhesive material for drug delivery systems



Sabrina Dias Ribeiro<sup>a,b,\*</sup>, Guimes Rodrigues Filho<sup>a</sup>, Andréia Bagliotti Meneguim<sup>c</sup>, Fabíola Garavello Prezotti<sup>c</sup>, Fernanda Isadora Boni<sup>c</sup>, Beatriz Stringhetti Ferreira Cury<sup>c</sup>, Maria Palmira Daflon Gremião<sup>c</sup>

<sup>a</sup> Federal University of Uberlândia, Chemistry Institute, Uberlândia, Minas Gerais, Brazil

<sup>b</sup> Federal University of Uberlândia, Integrated Sciences College of Pontal (FACIP), Ituiutaba, Minas Gerais, Brazil

<sup>c</sup> State University Paulista Júlio de Mesquita Filho, Araraquara, São Paulo, Brazil

## ARTICLE INFO

### Article history:

Received 21 March 2016

Received in revised form 9 July 2016

Accepted 17 July 2016

Available online 19 July 2016

### Chemical compounds studied in this article:

Ketoprofen (PubChem CID: 3825)

Cellulose triacetate (PubChem CID: 44263853)

### Keywords:

Cellulose triacetate

Gellan gum

Coating

Mucoadhesive

Controlled release

Ketoprofen

## ABSTRACT

Cellulose triacetate (CTA) films were produced from cellulose extracted from sugarcane bagasse. The films were characterized using scanning electron microscopy (SEM), water vapor permeability (WVP), mechanical properties (MP), enzymatic digestion (ED), and mucoadhesive properties evaluation (MPE). WVP showed that more concentrated films have higher values; asymmetric films had higher values than symmetric films. MP showed that symmetric membranes are more resistant than asymmetric ones. All films presented high mucoadhesiveness. From the WVP and MP results, a symmetric membrane with 6.5% CTA was selected for the coating of gellan gum (GG) particles incorporating ketoprofen (KET). Thermogravimetric analysis (TGA) showed that the CTA coating does not influence the thermal stability of the particles. Coated particles released 100% of the KET in 24 h, while uncoated particles released the same amount in 4 h. The results highlight the CTA potential in the development of new controlled oral delivery systems.

© 2016 Elsevier Ltd. All rights reserved.

## 1. Introduction

The oral route represents a simple, secure and comfortable way for drug administration and these features make it the most used route worldwide (Lopes, Bettencourt, Rossi, Buttini, & Barata, 2016; Mu, Holm, & Müllertz, 2013; Varum, Hatton, & Basit, 2013).

**Abbreviations:** CTA, cellulose triacetate; DT, dissolution test; DTA, differential thermal analysis; EB, elongation at break; ED, enzymatic degradation; GG, gellan gum; GIT, gastrointestinal tract; KET, ketoprofen; MC, microcapsules; MP, mechanical properties; MPE, mucoadhesive properties evaluation; NSAID, non-steroidal anti-inflammatory drug; PS, puncture strength; SEM, scanning electron microscopy; SI, swelling index; TGA, thermogravimetric analysis; WVP, water vapor permeability.

\* Corresponding author at: Federal University of Uberlândia, Integrated Sciences College of Pontal (FACIP), Ituiutaba, Minas Gerais, Brazil.

E-mail addresses: [sabrinaquimica@yahoo.com.br](mailto:sabrinaquimica@yahoo.com.br) (S.D. Ribeiro), [guimes.rodriguesfilho@gmail.com](mailto:guimes.rodriguesfilho@gmail.com) (G. Rodrigues Filho), [abagliottim@hotmail.com](mailto:abagliottim@hotmail.com) (A.B. Meneguim), [fasuecia@yahoo.com.br](mailto:fasuecia@yahoo.com.br) (F.G. Prezotti), [boni.fernanda@gmail.com](mailto:boni.fernanda@gmail.com) (F.I. Boni), [curybsf@fcfar.unesp.br](mailto:curybsf@fcfar.unesp.br) (B.S.F. Cury), [pgremiao@uol.com.br](mailto:pgremiao@uol.com.br) (M.P.D. Gremião).

However, many drugs present problems related to absorption, solubility and/or permeability in the upper parts of the gastrointestinal tract (GIT), resulting in low bioavailability if given orally (Meka, Dharmanlingam, & Kolapalli, 2014; Mizoguchi et al., 2015). The drugs stability in acidic conditions can be another important tissue that limits the use of this route.

The low aqueous solubility of some drugs as those belonging to BCS Class II, which represent about 40% of marketed drugs, imposing a great challenge for the design of oral drug delivery systems because this lack of solubility may prevent a sufficient drug concentration to reach the absorption site, harming the bioavailability (Babu & Nangia, 2011; Löbenberg & Amidon, 2000). In this way, different strategies as hydrophilic solid dispersion (Chan, Chung, Cheah, Tan, & Quah, 2015; Włodarski et al., 2015) phospholipidic solid dispersion (Fong, Ibisogly, & Bauer-Brandt, 2015; Shende, Gaud, Bakal, & Patil, 2015), cyclodextrin inclusion complex (Maestrelli, Zerrouk, Cirri, Mennini, & Mura, 2008) and nanosuspensions (Wang, Han, Wang, & Wang, 2016; Xia et al., 2010) have been exploited in order to improve the dissolution rates and so, the oral absorption of such drugs

KET is a common model of poorly water-soluble and non-steroidal anti-inflammatory drug (NSAID), commonly used for the treatment of rheumatoid arthritis (Maestrelli, Zerrouk, Cirri, & Mura, 2015; Perontis, Hatzidimitriou, Begou, Papadopoulos, & Psomas, 2016). Several studies are designed to improve the therapeutic effectiveness of KET (Belkacem, Salem, & AlKhatib, 2015; Boni, Prezotti, & Cury, 2016; Chan et al., 2015; Gue et al., 2013; Maestrelli et al., 2015; Yu et al., 2016).

In this context, the development of modern solid dosage forms to improve the stability, solubility, premature release, absorption and/or permeability of drug, is a rational approach to increase therapeutic effectiveness when drugs are administrated orally. Mucoadhesive and coating technologies are alternative to overcome these problems (Meka et al., 2014; Varum et al., 2013).

Coating is an important technological tool that has been widely used in the solid dosage forms manufacturing for a variety of reasons. Drug protection against environmental factors such as humidity, light and gases, taste or odor masking, increasing the swallowing ease and the improving mechanical strength are some of the functions that can be improved by coating the product. Polymer coatings can be successfully used to control and/or modify the patterns of drug release in the design of new controlled drug delivery systems (Maroni, Del Curto, Zema, Foppoli & Gazzaniga, 2013; Meneguín, Cury, & Evangelista, 2014; Prezotti, Meneguín, Evangelista, & Cury, 2012).

Bio/mucoadhesive polymeric systems represent a promising tool for achieving site-specific drug delivery because the bioadhesion allows the immobilization of a drug in the action/absorption site for extended times, establishing a close contact with the epithelium. In such way, the absorption and bioavailability of several drugs can be improved (Caccavo, Lamberti, Cascone, Barba, & Larsson, 2015; Zhang, Chan, Moretti, & Urich, 2015).

Cellulose esters have been used in the development of new drug delivery systems such as microspheres, solid dispersions and films, with the purpose of controlling drug diffusion rates, especially in the GIT (Fonseca et al., 2015; Kajjari, Manjeshwar, & Aminabhavi, 2014; Liakos et al., 2016; Rodrigues Filho et al., 2011, 2015; Sosnik, Neves, & Sarmento, 2014; Zhang et al., 2015).

Among the cellulose esters, cellulose acetate arouses particular interest because of its biocompatibility, biodegradability, non-toxicity and low cost (Sosnik et al., 2014; Yu et al., 2013). The use of cellulose acetate as a membrane for coating or drug incorporation has recently been reported (Milovanovic et al., 2016; Rodrigues Filho et al., 2011, 2015; Ruggiero et al., 2015; Yu et al., 2013).

In this study free films of cellulose triacetate from sugar cane bagasse were prepared by casting film method. The free films were characterized by scanning electron microscopy (SEM), water vapor permeability (WVP), mechanical properties (MP), swelling index (SI), dissolution test (DT), enzymatic degradation (ED) and thermogravimetric analysis (TGA). CTA film was used to coat cross-linked GG microspheres incorporated with KET and its mucoadhesion and *in vitro* dissolution properties were evaluated to predict the performance of such film coatings in controlled drug delivery systems.

## 2. Experimental

### 2.1. Delignification of bagasse, acetylation and characterization

Sugarcane bagasse was delignified, later acetylated and characterized according to a previously described method (Rodrigues Filho et al., 2011).

**Table 1**

Composition of solutions used in membranes preparation.

Membranes	CTA (g)	Dichloromethane (mL)	Water (mL)
1	0.3	10.0	0.0
2	0.65	10.0	0.0
3	1.0	10.0	0.0
4	0.3	9.0	1.0
5	0.65	9.0	1.0
6	1.0	9.0	1.0

### 2.2. Production of membranes

Membranes were produced by the casting method (Rodrigues Filho et al., 2015). Dispersions with different CTA concentrations, dichloromethane and amounts of water were prepared according to Table 1. The dispersions were stirred for 24 h at 50 rpm in a mechanical stirrer and further spread on a glass plate with the aid of a spreader, solvent evaporation occurred freely at 25 °C for 10 min.

### 2.3. SEM

Membrane surfaces and fractures were analyzed by SEM at the Chemical Engineering College at the Federal University of Uberlândia (FEQ-UFU). The equipment used was a Carl Zeiss model EVO 10 MA scanning electron microscope. Fractures were obtained through breakage in liquid nitrogen. The samples were metalized with a thin gold layer. Analyses of the microcapsule surfaces with and without coating were carried out in scanning electron microscope model EGF-SEM KAL 6330F, at State University Paulista-UNESP/Araraquara.

### 2.4. Water vapor permeability (WVP) of free films

WVP was tested according to a standard protocol ASTM E96 and Komatsu, Otaguro, and Ruvolo Filho (2014). In a Payne's cup 10 mL of distilled water was added. The closing of cup was performed through a system where the polymeric film was placed between two rubber rings. The ensemble was then placed in a desiccator in the presence of a desiccant agent (phosphorus pentoxide), with the purpose of generating relative humidity gradient between the interior of the cup and the interior of the desiccator. This way, this pressure gradient generated within the desiccator allows the water vapor permeation through the polymer film. Initially the Payne's cups were weighted in short time intervals, posteriorly to larger intervals as the mass variation decreases. This variation is directly proportional to the water vapor that passes through the polymer film. The experiment was performed in triplicate. The flow  $J$  and permeability  $P$  of water vapor were calculated using the Eqs. (1) and (2), respectively, as follows:

$$J = \Delta m / \Delta t \times A \quad (1)$$

where  $\Delta m / \Delta t$  is the angular coefficient of the mass variation versus time graph, obtained from the measurements of Payne's cups and  $A$  is the area of polymeric film exposed during the test.

$$P = J \cdot L / \Delta P_V(T) \quad (2)$$

where  $J$  is the water vapor flow calculated from Eq. (1),  $L$  is the membrane thickness and  $\Delta P_V(T)$  is the difference in vapor pressure at a given temperature.

### 2.5. Mechanical properties (MP) of free films

Mechanical properties of free films were evaluated on a texture analyzer TA-XT2 (Stable Mycro-Systems) using a spherical-ended puncture probe ( $D = 25$  mm). Samples ( $n = 6$ ) were attached on a

metallic holder with circular hole ( $D = 5$  cm) and the probe moved down at  $1 \text{ mm s}^{-1}$  to film surface and during the test the velocity was  $0.10 \text{ mm s}^{-1}$ . The trigger force was  $0.005 \text{ kg}$ . Curves of force versus displacement were recorded until the film rupture and used to determine its mechanical properties, such as puncture strength (PS) and elongation at break (EB) according to Eqs. (3) and (4), respectively (Meneguín et al., 2014; Prezotti et al., 2012).

$$Ps = F/A \quad (3)$$

where  $F(N)$  is the force required to film rupture and  $A(m^2)$  is the sectional area of the films, calculated from  $A = 2rh$ , where  $r$  is the hole radius and  $h$  is the film thickness.

$$Ep = \frac{\sqrt{r^2 + d^2} - r}{r} \times 100 \quad (4)$$

where  $r$  (mm) is the radius of exposed film and  $d$  is the displacement.

## 2.6. Mucoadhesive properties evaluation (MPE) of free films

The mucoadhesion test of free films was carried out on a texture analyser TA-XT2 (Stable Mycro-Systems) with 50 N load cell by measuring the force required to remove the samples from a mucin disc type II (maximum detachment force,  $F_{MA}$ ) and the work involved in the mucoadhesion process ( $W_{MA}$ ). Film sections were fixed at the cylindrical probe (10 mm) and the mucin disc ( $0.95 \text{ cm}^2$ ) was attached to metallic holder, both using double-sided adhesive tape. Mucin discs were hydrated with 0.1 M phosphate buffer (pH 7.4) and the solution excess was removed with an absorbent paper. Then, the probe was moved down ( $0.5 \text{ mm s}^{-1}$ ) until the contact with mucin disc (contact time = 100 s). The probe was subsequently withdrawn at constant speed of  $0.5 \text{ mm s}^{-1}$ . The  $F_{MA}$  and  $W_{MA}$  were obtained with the aid of the Texture Exponent Lite software.

## 2.7. Enzymatic digestion of free films (ED)

Films sections (100 mg) were placed in contact with 2 mL of 0.1 M phosphate buffer (pH 7.1) for 30 min at  $100^\circ\text{C}$ . After, the films were incubated with pancreatin enzymatic solution ( $0.15 \text{ g mL}^{-1}$ ) at  $37^\circ\text{C}$  for 180 min. Aliquots were withdrawn at predetermined times and the enzymatic activity was stopped with 80% ethanol (v/v) addition. Digested content (%) was quantified spectrophotometrically in UV-vis Spectrophotometer Hitachi at 540 nm after reaction with 3,5-dinitrosalicylic acid (Bernfeld, 1955; Meneguín et al., 2014).

## 2.8. Dissolution test of free films

Dissolution studies were performed according to Meneguín et al. (2014). Dissolution studies were performed on a Hanson Research (New Hanson SR-8 plus) dissolution station, using apparatus USP V (USP 37). Films section ( $4 \text{ cm}^2$ ) were fixed on the transdermal patch holder (17 mesh) and accurately weighed. The set was placed on bottom of the dissolution vessels containing 0.1 N HCl (pH 1.6) or 0.1 M phosphate buffer (pH 7.4) at  $37^\circ\text{C}$  and stirred at 50 rpm for 120 and 180 min, respectively. After that, the films were removed and dried on an oven-drier until constant weight. The films dissolution was gravimetrically determined.

## 2.9. Swelling index (SI)

Swelling index studies were carried out according to Moustafine, Zaharov, and Kemenova (2006) and Nep, Asare-Addo, Ghori, Conway, and Smith (2015). A sample of the membrane was immersed into 40 mL of HCl 0.1 N (pH 1.6) solution for 1 h at  $36.5^\circ\text{C}$ . After removed from acid solution, the sample was

immersed into 40 mL of 0.1 M pH 7.4 solution for 23 h at  $36.5^\circ\text{C}$ . Throughout the experiment the membrane was removed from the fluids, wiped with absorbent and weighed periodically.

## 2.10. Preparation of gellan beads containing KET

The beads were prepared by the ionotropic gelation method as previously proposed (Boni et al., 2016; Prezotti, Cury, & Evangelista, 2014). Briefly, an aqueous dispersion of gellan gum (2.0% w/v) was prepared under magnetic stirring at  $60^\circ\text{C}$ . KET (1% w/v) was added under constant stirring for homogenization. The dispersions were dripped into the cooled ( $4^\circ\text{C}$ ) crosslinking solution containing aluminum chloride 5% (w/v) using syringe and flat-tipped needles (23G) and the set was kept under stirring for 20 min to complete the crosslinking reaction. The microspheres were separated by filtration, washed with distilled water and dried at room temperature until constant weight.

## 2.11. CTA film coating of GG microcapsules (MC)

Based on the results of WVP and PS, gellan MC were coated using filmogenic dispersion 2, which was prepared by dispersing 0.65 g of CTA in 10 mL of dichloromethane under magnetic stirring (50 rpm) and until complete homogenization. MC (500 mg) were immersed in this filmogenic dispersion and stirred for 5 min. The MC were then filtered and dried at room temperature.

## 2.12. Thermogravimetric analysis (TGA) and differential thermal analysis (DTA)

TGA experiments were performed in a DTG 60-H, Shimadzu. Seven milligrams of the samples were heated from room temperature to  $600^\circ\text{C}$  at a rate of  $10^\circ\text{C min}^{-1}$  under nitrogen atmosphere. DTA experiments were carried out simultaneously under same conditions.

## 2.13. Ex vivo mucoadhesion test

The *ex vivo* mucoadhesion test was performed with fresh porcine large intestine tissue as previously described by Prezotti et al. (2014) and Boni et al. (2016). Briefly, the beads were carefully placed on the tissue and a previous contact time (20 min) was allowed. After this, the tissue was rinsed with phosphate buffer pH 6.0 ( $30 \text{ mL min}^{-1}$ , for 5 min). The mucoadhesiveness was expressed as the percentage of beads that remained adhered to the tissue at the end of the test.

## 2.14. In vitro drug release

KET release analysis from CTA coated GG beads were performed on a Hanson Research Dissolution Test Station SR8-Plus (Chatsworth, USA) equipped with the USP apparatus I (basket) at 50 rpm and  $37 \pm 0.4^\circ\text{C}$ . The first step of the dissolution test was carried out in 750 mL of acid media (0.1 N HCl, pH 1.2), containing sodium lauryl sulfate (0.75%) as surfactant due to low solubility of KET in this medium, for 2 h. For next step, the pH was adjusted to 7.4 by adding 0.2 M tribasic sodium phosphate, completing 900 mL of media and the test was conducted for 4 h. After this, the pH was changed for 6.0, using 2 N HCl. At predetermined times aliquots were withdrawn and the KET release was quantified on a spectrophotometer at 258 nm for the acid pH and 260 nm for both pH 6.0 and 7.4. The volume of dissolution media withdrawn at each sampling was immediately replaced with same volume of media at the same temperature to maintain the sink condition. Beads containing 150 mg of KET were tested in triplicate.

### 2.15. Statistical analysis

One-way analysis of variance (ANOVA) followed by a Tukey test was used to evaluate significant differences. A significance level of 5% was adopted.

## 3. Results and discussion

### 3.1. Characterization of bagasse and CTA

Delignified bagasse is composed of 87.59% cellulose, 12.00% hemicellulose and 0.41% lignin. The cellulose acetate presents a substitution degree of  $2.80 \pm 0.09$  and is classified as cellulose triacetate and a viscosity average molecular weight of  $39,000 \text{ g mol}^{-1}$  (Rodrigues Filho et al., 2011).

### 3.2. SEM

The membrane structure has an influence on several properties (mechanical, WVP, diffusion and drug release). The morphologies of the produced membranes are shown in Fig. 1A and B.

In the micrographs seen in Fig. 1A, a structure without pores can be observed. In the surface, as well as in the cross-section, a dense morphology can be seen. Given these observations, membranes 1–3 were classified as symmetric.

The technique used in the production of the membranes was casting film method. Solutions were prepared with different concentrations of dichloromethane (solvent) and CTA (polymer). After homogeneous solutions were achieved, they were spread and the solvent evaporated freely. This step promotes the formation of polymer-rich regions.

Different CTA concentrations did not change the morphology of the membranes, only the thickness. Membrane 1 was thinner than the others, as seen in the micrographs, which are at the same magnification. This was caused by the lower amount of polymer present in the solution.

In contrast to Fig. 1A, membranes 4–6 (Fig. 1B) have pores in their structures, as seen in cross-section. The pores have heterogeneous forms and distribution. Membranes 4–6 were thus classified as asymmetric.

The method used in the preparation of asymmetric membranes was the same as for the symmetric ones, but with water added in the mixture that in this situation is a non-solvent. There is the formation of dispersion due to the immiscibility of water and dichloromethane. When spread on the glass slide, both the dichloromethane and the water evaporate freely. However, dichloromethane has greater volatility than water, and this allows quicker evaporation. The water persistence in polymeric chains for a longer time interval causes a phase separation. Cellulose triacetate is hydrophobic, and therefore, in regions where there are water molecules, there is low-density polymer, resulting in the formation of pores.

There was pore formation regardless of the CTA percentage in the formulation. However, membrane 6 presents more uniform pores. The polymer/water ratio is greater in membrane 6, compared to the others. A larger proportion of polymer decreases the extent of the phase separation, consequently forming smaller and more uniform pores.

### 3.3. WVP

WVP testing yields information about the water vapor transport and barrier capacity of the membranes. Table 2 shows the values obtained for thickness and WVP of the membranes.

Different concentrations and morphology produced significant differences in the WVP results ( $p < 0.05$ ). The WVP values increased

proportionately with the CTA concentration, and consequently with the thickness. In asymmetric membranes WVP values were higher than for the symmetric membranes, except for the membranes prepared with 10% CTA.

The barrier capacity of a polymeric film is essential information in choosing polymers for the development of controlled drug release systems, because the coating should protect the formulation from moisture in the environment during storage. Materials showing resistance to water vapor permeability are desirable for applications in the pharmaceutical industry (Mwesigwa & Basit, 2016). Therefore, in this study the most suitable membranes for the protection of pharmaceuticals against the passage of water vapor are samples 1 and 2 due to their smaller WVP values.

### 3.4. MP

In order to obtain effective coating of solid dosage forms film, the coatings should present enhanced mechanical and barrier properties, without being brittle (Heinämäki et al., 2015). Data on PS and EB at break of the CTA films are shown in Table 2.

The PS and EB values show that all of the films presented a similar trend, such that these parameters were dependent on the CTA concentration and morphology. Increasing of the CTA concentration from 3% to 6.5% enhanced the mechanical properties, with an increase in the values of PS (about 11.8x and 9.2x) and EB (3.5x and 4.5x) for symmetric and asymmetric films, respectively. This behavior is indicative that when higher polymer concentrations are used, more packed structures with entangled polymeric chains are produced, which are stronger and support higher forces before rupture.

However, the raising of CTA concentration from 6.5% to 10% in symmetric films did not cause a significant improvement in mechanical properties ( $p > 0.05$ ) and for asymmetric membranes the increase was less pronounced (about 2.1x for PS and 1.2x for EB) when compared with 3 and 6.5% films. This trend suggests that the intermediate polymer concentration (6.5%) produced structures that were compact enough to withstand perforation, but at the same time, with large intermolecular spaces that should allow an extensive structural rearrangement due to the force application before the yield point is reached (Felton, 2007). At higher concentrations, more dense packing of the polymer chains occurs contributing to stronger intermolecular interactions, resulting in a less flexible and more brittle film.

Concerning the system morphology, symmetric films presented improved mechanical properties compared with asymmetric films. This behavior can be related to the building of a homogeneous matrix structure without the presence of pores, which unlike the intermolecular spaces, represent less dense regions that increase the distance between polymer chains, decreasing their interactions and facilitating perforation.

### 3.5. MPE

Information about the mucoadhesive properties of dosage forms intended for oral, buccal or nasal administration is an important tool for assessing the ability of these systems to increase rates of permeation and absorption across the epithelial membrane, thus enhancing bioavailability. More intimate contact for a longer time established by the interpenetration of polymer and mucin chains also favors the creation of local gradients of concentration (Ameje et al., 2002). The polymers properties are crucial for establishment of the mucoadhesion process. Data on mucoadhesion force and adhesion work are summarized in Table 2.

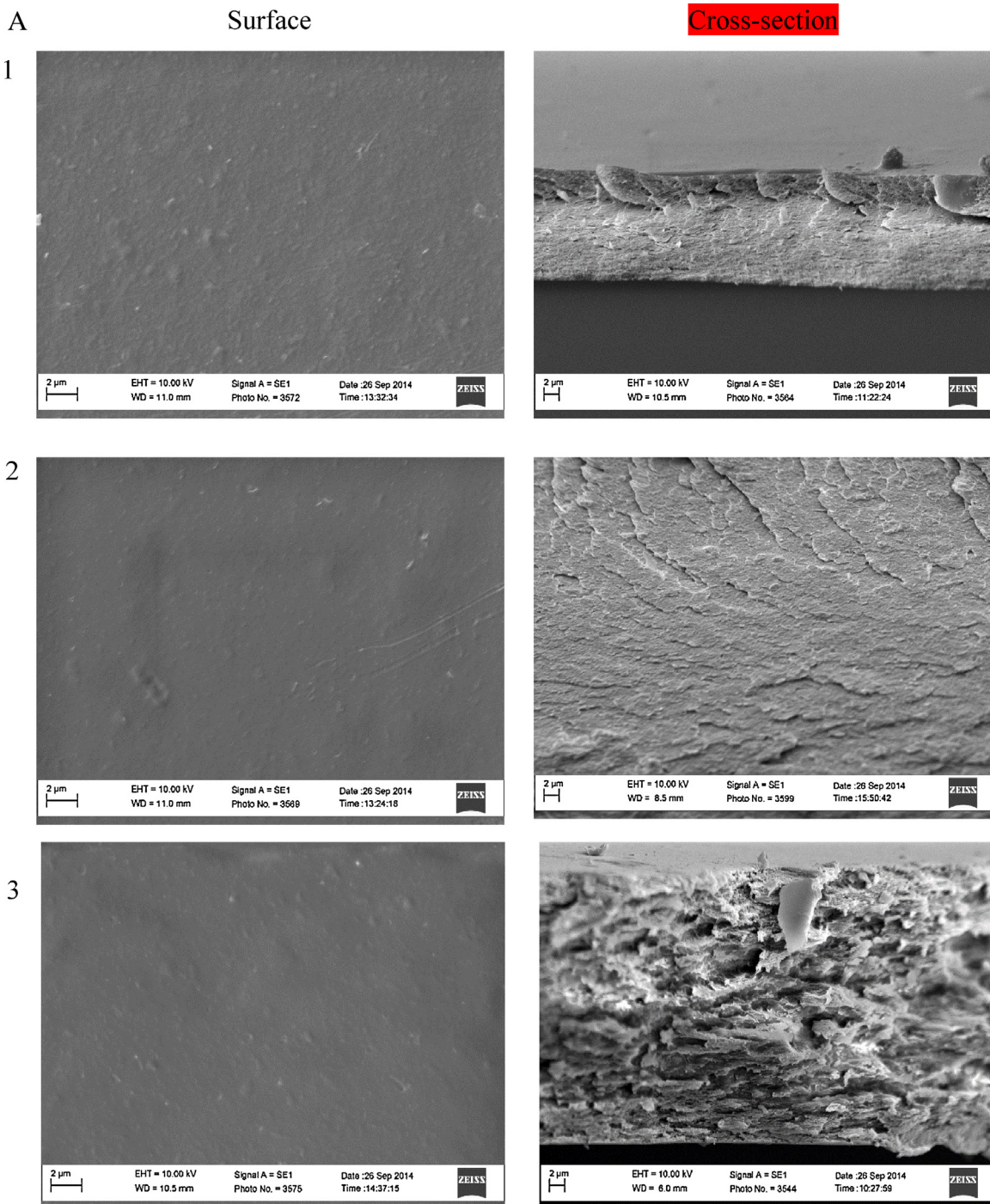
The mucoadhesive properties were evaluated by measuring the maximum detachment force ( $F_{MA}$ ) and adhesion work ( $W_{MA}$ ). High values of  $F_{MA}$  (up to 6.9 N) and  $W_{MA}$  (3.4 N/s) revealed that the CTA



**Table 2**

WVP values, the thickness, mechanical properties, maximum detachment force, work of adhesion of the CTA films.

Morphology	Samples	CTA Concentration (%)	WVP ( $10^{-3}$ g mm min $^{-1}$ m $^{-2}$ KPa $^{-1}$ )	Thickness (mm)	Puncture Strength (PS) (MPa)	Elongation at break (EB) (%)	Maximum detachment force (N)	Work of adhesion (N/s)
Symmetric	1	3	$1.5913 \pm 0.1153$	$0.01016 \pm 0.00072$	$7.8094 \pm 0.5879$	$0.7034 \pm 0.08244$	$5.9133 \pm 1.1040$	$2.5618 \pm 0.7290$
	2	6.5	$2.6634 \pm 0.4758$	$0.02082 \pm 0.00051$	$91.6339 \pm 12.0214$	$2.4710 \pm 0.2854$	$5.9493 \pm 0.4378$	$2.3205 \pm 0.5796$
	3	10	$4.8061 \pm 0.2678$	$0.03675 \pm 0.0025$	$106.5801 \pm 10.5226$	$2.7395 \pm 0.4988$	$5.9138 \pm 0.9780$	$3.2978 \pm 0.5360$
Asymmetric	4	3	$3.3676 \pm 0.1126$	$0.01880 \pm 0.00072$	$1.6896 \pm 0.1568$	$0.2509 \pm 0.02434$	$5.6953 \pm 0.1786$	$3.4777 \pm 0.1530$
	5	6.5	$4.1450 \pm 0.5056$	$0.02616 \pm 0.0033$	$15.5879 \pm 2.2053$	$1.1328 \pm 0.1697$	$6.9068 \pm 0.5355$	$3.0635 \pm 0.1993$
	6	10	$4.4112 \pm 0.2569$	$0.03404 \pm 0.0033$	$32.8626 \pm 8.4762$	$1.4015 \pm 0.2035$	$5.9750 \pm 0.3993$	$3.1455 \pm 0.6955$

**Fig. 1.** (A) SEM of membranes 1, 2 and 3. Surface (10,000 $\times$ ) and fractures (5000 $\times$ ) and (B) SEM of membranes 4, 5 and 6. Surface (10,000 $\times$ ) and fractures (5000 $\times$ ).

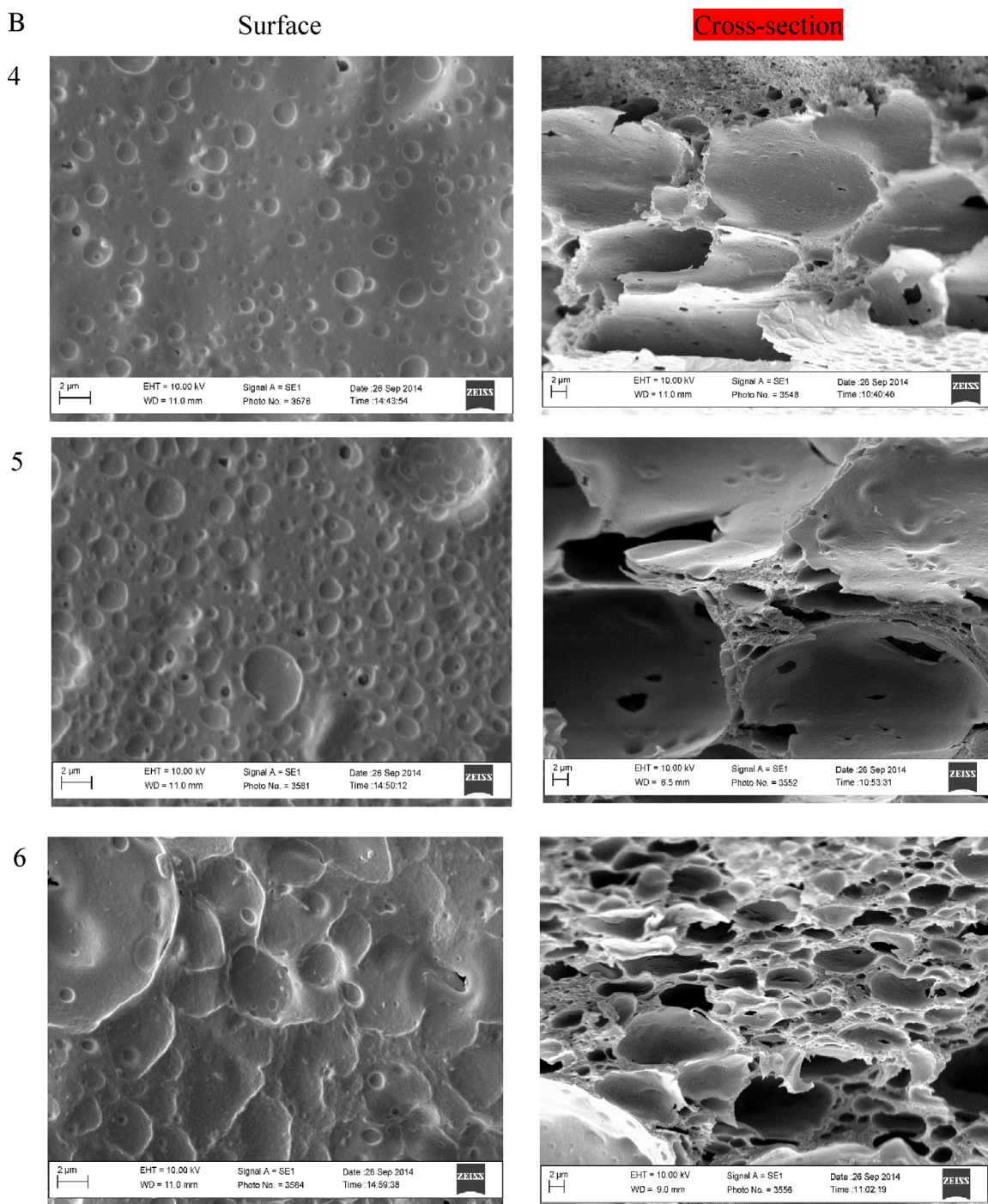


Fig. 1. (Continued)

films, regardless of the polymer concentration or morphology, have a high capacity for adhesion to the mucosa.

Mucoadhesion is discussed to a large extent in the literature and its mechanism is not fully explained yet. There are several papers discussing the factors that influence mucoadhesive forces (Carvalho, Chorilli, & Gremião, 2014; Sosnik et al., 2014). Electronic, adsorption, diffusion, swelling and fracture theories have been used to attempt to explain the process. In some cases, a combination of several theories can be helpful in understanding the mucoadhesive process.

Mucus is composed of glycoproteins, lipids, inorganic salts and water. Mucin is a glycoprotein with large amounts of serine, threonine, and proline. It has a complex molecular structure, with functional groups such as amines, carboxyl and hydroxyl groups, and amides (Carvalho et al., 2014). Cellulose triacetate is a polymer containing acetyl and hydroxyl groups. Considering the polymer and mucin properties, the theory that best explains mucoadhesion is adsorption, being based on the presence of hydrogen bonds and Van der Waals forces (Smart, 2005).

Previous research reports the use of a method based on force detachment (Eouani, Piccerelle, Prinderre, Bourret, & Joachim,



2001) to evaluate the mucoadhesive performance of the polymers carbopol 971 P and sodium carboxymethyl cellulose. They evaluated the mucoadhesive force as a function of contact time. After the longest contact period, 30 min, the values obtained were 4.47 and 0.49 N, respectively. Another study evaluated the mucoadhesive performance of poloxamer 407 and carbopol 934 and the values found were 0.39 and 0.28 N, respectively, with a contact time of 15 min (Bruschi et al., 2007).

These results show that cellulose triacetate has great potential to be used as mucoadhesive, since it exhibits larger values of mucoadhesive force, compared with other polymers used in the literature.

### 3.6. ED

Among other functions, film coatings can offer additional protection to solid pharmaceuticals dosage forms against the enzymatic degradation that occurs in the upper portions of the gastrointestinal tract, as well as having an important role in the targeting of drugs to specific organs or tissues. Coating materials intended to protect proteins or peptides, or those intended for colon specific release should exhibit low solubility in acid media, which corresponds to the gastric environment, and high resistance against enzymatic degradation in the anterior portions of the colon (Drechsler, Garbacz, Thomann, & Schubert, 2014).

A test of enzymatic digestion using pancreatin – a complex enzyme that comprises amylase, lipase and protease – was performed to simulate digestion in the small intestine in order to evaluate the protective ability of the CTA films (Freire, Podczec, Veiga, & Sousa, 2009). Table 3 shows the percentage of digested CTA after incubation with  $\alpha$ -amylase pancreatic solution based on amount of glucose released over time.

In general, all films were quite resistant to enzymatic degradation with the percentage of digested CTA ranging from 2.7 to 6.8% after 180 min, meaning that there was a protection of up to 97% by the coating material.

As expected, increased CTA concentration reduced the degree of enzymatic digestion, since a higher polymer mass is available for degradation. Moreover, the most entangled state of polymer chains likely hampers the access of the enzymes to the glycosidic bonds.

In relation to the morphology of the films, asymmetric films were less susceptible to digestion (up to 34%) than the symmetric ones. Although the former have pores homogeneously distributed throughout the polymer network that from small channels through which liquids and other substances can spread more easily, these films likely possess a greater flexibility in their polymeric chains, which allows reorganization of the network, restricting enzymatic digestion (Meneguín et al., 2014).

Considering that the pancreatin is present in the key digestion processes that occurs in small intestine, these results suggest that the CTA films can be considered a promising material for targeting drugs to the colon.

### 3.7. DT and SI

Based on the previous testing, sample 2, which contains 6.5% of CTA, was chosen to test as a coating for gellan particles. The choice was made based on the results of WVP and MP, in which concentration and morphology exerted significant influence on the results obtained. The WVP results showed that symmetric membranes with lower CTA concentrations are less permeable to water vapor and the PS values showed that the symmetric membrane with 6.5% CTA offered the best performance. The coating of a microcapsule is important in many areas, ranging from aesthetic effects to improving pharmaceutical performance. Given this, it is extremely important to know the behavior of the polymer used, to test it

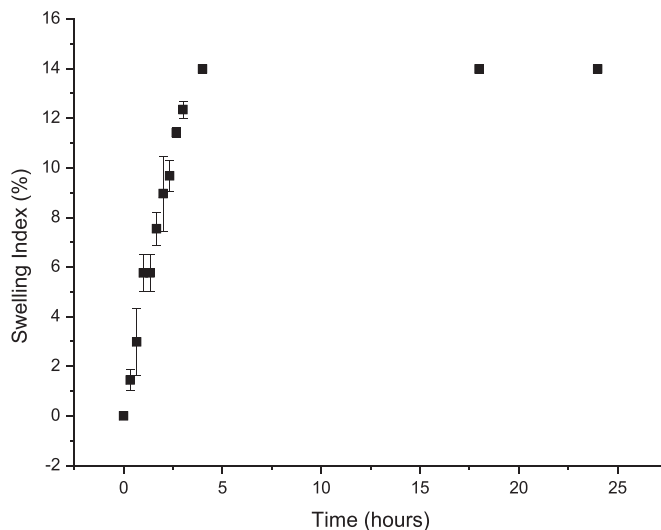


Fig. 2. Swelling index of the membrane used in the coating.

in ways that simulate the gastrointestinal tract, and to assess its hydration capacity.

The selected film showed 2.01% dissolution at acidic pH (1.2) and 1.34% at a basic pH (7.4). The swelling index of the CTA membrane in acidic and basic media is displayed in Fig. 2.

The dissolution results show a small amount of CTA membrane dissolved in acid and basic medium. The values observed in Fig. 2, indicate similar behavior related to the water absorption. During the first hour of the experiment, when the membrane was immersed in an acidic medium, the SI increased gradually. From the second hour at neutral pH, the SI continued to rise for 2 h and then remained constant at approximately 14%.

The SI and the dissolution percentage are properties related to the polymer characteristics. CTA has hydrophobic character and is therefore insoluble in water, which hampers the water penetration into the polymeric chains and also the dissolution of the chains in aqueous medium.

Both results are important for the application of a material as coating. A pharmaceutical formula that will act in the intestine needs gastric protection, therefore it is desirable that the material used for coating is resistant to acid medium, as was the case for CTA.

The swelling index is very important in the study of polymeric matrixes, as it assesses the ability of a polymer to become hydrated, a very important property in drug release kinetics. A value for the swelling index may represent the first step in the development of mathematical models suitable for designing controlled drug release kinetics (Mundargi, Patil, & Aminabhavi, 2007; Prezotti et al., 2012).

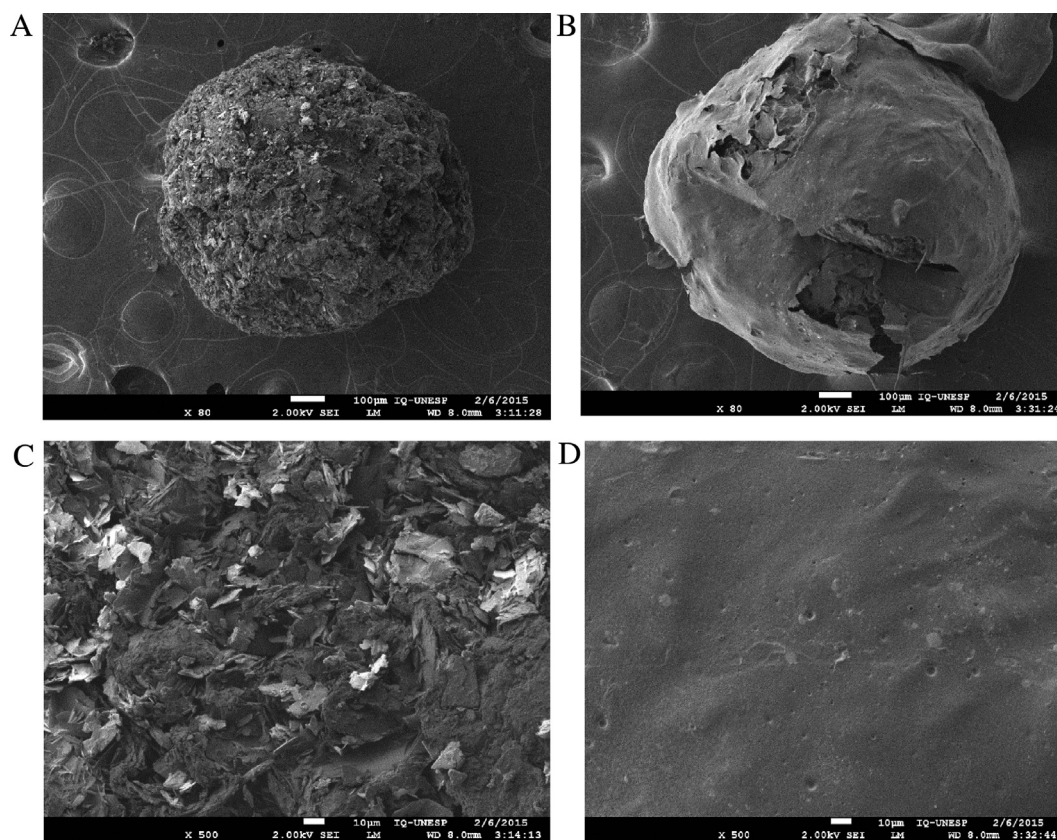
### 3.8. Coating of gellan particles with CTA membrane

The coating was performed using the immersion method with subsequent drying. Gellan particles without and with coating are shown in Fig. 3.

Fig. 3A and B shows the particles without and with coating. Uncoated particles present a porous structure and are uneven, as noted previously by other authors (Prezotti et al., 2014). In this report, the authors observed that the heterogeneous particle morphology of gellan gum is due to the presence of the drug KET, which is inserted between the polymer chains causing disorder in the structure. Coated particles showed a surface with a dense morphology, which is due to the presence of the CTA film formed during coating. This difference in morphology is shown in Fig. 3C and D.

**Table 3**  
Enzymatic digestion values over time (%).

Samples		Enzymatic digestion (%)				
Morphology	CTA (%)	20 min	60 min	120 min	150 min	180 min
Symmetric	3	0.331 ± 0.014	1.535 ± 0.115	3.762 ± 0.519	5.772 ± 0.421	6.796 ± 0.259
	6.5	0.768 ± 0.239	1.478 ± 0.011	2.611 ± 0.146	3.399 ± 0.003	4.274 ± 0.071
	10	0.513 ± 0.043	0.843 ± 0.051	1.284 ± 0.227	2.052 ± 0.032	2.988 ± 0.005
Asymmetric	3	0.976 ± 0.255	2.075 ± 0.088	2.599 ± 0.188	3.933 ± 0.078	4.439 ± 0.011
	6.5	0.675 ± 0.290	1.13 ± 0.018	1.839 ± 0.013	2.427 ± 0.031	2.949 ± 0.066
	10	0.654 ± 0.111	0.923 ± 0.093	1.367 ± 0.278	1.984 ± 0.009	2.711 ± 0.234

**Fig. 3.** SEM of particles without and with coating, A and B, respectively at 80× magnification. SEM of particle surface of uncoated particle (C) and coated particle (D).

### 3.9. TGA and DTA

In this work, the thermal analysis was used to examine the influence of coating with CTA on the thermal properties of the gellan particles. TGA and DTA curves are seen in Fig. 4.

In Fig. 4, mass variation curves as a function of temperature for particles with and without coating are presented. The thermal events are similar in both curves.

In both DTA curves, discrete endothermic peaks are observed at about 80 °C, which are assigned to the KET fusion (Prezotti et al., 2014).

At approximately 100 °C, about 10% mass loss is observed, which is assigned the desorption of water present on the GG and also on the CTA. This event is confirmed in the DTA curves, where a peak is observed at approximately 100 °C.

From 150 °C thermal decomposition of the polymer chains of the GG begins (approximately 40% of mass loss), followed by degradation of the KET (Prezotti et al., 2014). These events are also observed in the DTA curves.

The TGA curves presented differences only in the range between 250 and 350 °C. The particles coated with CTA showed lower mass loss in relation to the sample without coating. At 300 °C the coated particles lost approximately 50% of their mass, while the uncoated ones presented a loss of 56%. These thermal analysis results show that the presence of the CTA does not significantly influence the thermal stability of GG particles.

### 3.10. Ex vivo mucoadhesion test

At the end of the test, 100% of the coated microspheres remained strongly adhered to the porcine mucosa, demonstrating the high mucoadhesiveness of the beads (Prezotti et al., 2014).

### 3.11. In vitro release

The dissolution profile of KET from the coated and uncoated GG microspheres is presented in Fig. 5.



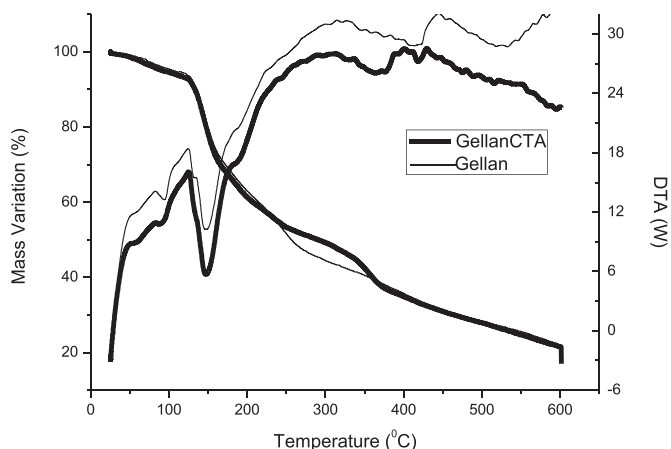


Fig. 4. TGA and DTA curves of gellan gum particles incorporating KET with and without coating.

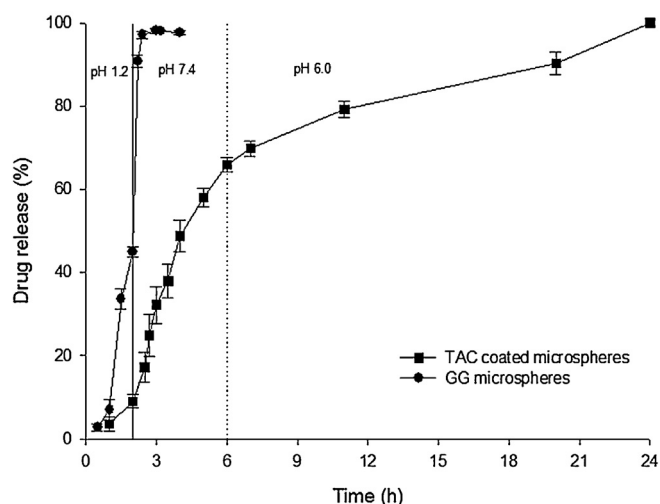


Fig. 5. Profile of *in vitro* release of KET from coated and uncoated gellan gum microparticles coated with CTA.

In the first 120 min of the experiment, 8.9% of the drug was released in acid medium (pH 1.2). In phosphate buffer (pH 7.4), a burst effect was observed, so that in the same time (120 min), 39.83% of the drug was released and 65.9% was released after 360 min. With the change of dissolution medium to phosphate buffer at pH 6.0, 100% of the drug was released from the microspheres after 24 h of the experiment.

The KET dissolution rate in acid media was significantly lower (about 5.3 times) than that observed in a study with uncoated cross-linked gellan gum microspheres (Boni et al., 2016), evidencing the ability of the CTA coating reduce the KET release rate. Angadi, Manjeshwar, and Aminabhavi (2011) also found that the coating made with stearic acid in chitosan and gelatin microspheres, prepared by the emulsion cross-linking method, reduced the release burst effect of the drug isoniazid.

The matrix of the microspheres is composed of a hydrophilic polymer (gellan gum) that is able to absorb liquid (303%) and swell (Boni et al., 2016), allowing mobility of the polymer chains that favors liquid diffusion through the polymer matrix and thus drug dissolution and diffusion.

CTA membranes have hydrophobic characteristics as evidenced by their low enzymatic digestion and dissolution of free films.

Therefore the CTA films behaved as a constant physical barrier against the diffusion of liquid into the matrix and the diffusion of drug molecules into the dissolution medium. This effect was also observed in the study of Mundargi et al., 2007; where matrices with hydrophobic character showed lower drug release values.

In acid media, the very low liquid absorption ability of films (14%) likely promoted a slight relaxation of the polymer chains allowing the penetration of low amounts of liquid into the microspheres and starting the dissolution process, resulting in the low percentage of drug released.

In the next part of the test, in phosphate buffer pH 6.0, the continuous intake of liquid in polymer matrix likely promoted erosion of the microspheres (Boni et al., 2016) and this more porous structure favored both liquid intake and the drug release, resulting in the rising release rate in this media.

Additionally, in the phosphate buffer cracking of the CTA coating could occur due to the swelling and consequent expansion of polymer matrix, making the drug release faster.

Drug dissolution data were fitted with Hixon and Crowell, Higuchi, Peppas and Weibull mathematical models in order to evaluate the mechanism that is involved in the drug release process. According to the correlation coefficient ( $r^2$ ), the Weibull model correlated best with the drug release data.

According to this model (Eq. (5)), the value of exponent  $b$  indicates the drug release mechanism.

$$F = 1 - \exp(-at^b) \quad (5)$$

$F$  = amount of drug released;  $b$  = shape parameter,  $a$  = time parameter.

Values of  $b < 0.75$  indicate Fickian diffusion, values of  $0.75 < b < 1.0$  indicate non-Fickian diffusion and values of  $b > 1.0$  indicate a complex drug release mechanism (Cury, Castro, Klein, & Evangelista, 2009; Papadopoulou, Kosmidis, Vlachou, & Macheras, 2006). The  $b$  value of 0.769 indicates that the release mechanism of the drug from the polymer matrix followed a non-Fickian diffusion, in which drug diffusion and polymer chain relaxation contribute to the control of drug release in a similar way.

#### 4. Conclusion

Cellulose triacetate membranes obtained from sugarcane bagasse were produced and characterized by SEM, WVP, MP, and MPE. A symmetric membrane with 6.5% CTA was selected for the coating of gellan gum particles incorporating KET. The membrane showed low values for enzymatic digestion, water vapor permeability, dissolution and swelling, showing its potential for protecting pharmaceuticals. All of the CTA membranes showed mucoadhesive force values higher than those reported in the literature. The coating was observed in SEM images. The results of thermal analysis indicated that the presence of the CTA does not influence the thermal stability of gellan gum particles. Finally, investigation of controlled KET release showed that coated particles released 100% of the drug during 24 h, while similar particles without coating released the same amount in 4 h. According to kinetic studies, the mechanism of KET release corresponds to non-Fickian diffusion. The results obtained in this work show the potential of a material obtained from agroindustrial residues for use in the pharmaceutical industry, because of its barrier, coating and mucoadhesive properties.

#### Acknowledgments

The authors thank CAPES for the access to “Portal Periódicos”, to FAPEMIG for project CEX-APQ-01128/13 and to Chemical Engi-

neering College of the Federal University of Uberlândia for the use of the SEM. Ribeiro thanks CAPES for the scholarships.

## References

- Amey, D., Voorspoels, J., Foreman, P., Tsai, J., Richardson, P., Geresh, S., et al. (2002). *Ex vivo* bioadhesion and *in vivo* testosterone bioavailability study of different bioadhesive formulations based on starch-g-poly(acrylic acid) copolymers and starch/poly(acrylic acid) mixtures. *Journal of Controlled Release*, 79, 173–182.
- Angadi, S. C., Manjeshwar, L. S., & Aminabhavi, T. M. (2011). Stearic acid-coated chitosan-based interpenetrating polymer network microspheres: Controlled release characteristics. *Industrial & Engineering Chemistry Research*, 50, 4504–4514.
- Standard Test Methods for Water Vapor Transmission of Materials. American Society for Testing and Materials, ASTM E96.
- Babu, N. J., & Nangia, A. (2011). Solubility advantage of amorphous drugs and pharmaceutical cocrystals. *Crystal Growth & Design*, 11, 2662–2679.
- Belkacem, N., Salem, M. A. S., & Alkhatib, H. S. (2015). Effect of ultrasound on the physico-chemical properties of poorly soluble drugs: Antisolvent sonocrystallization of ketoprofen. *Powder Technology*, 285, 16–24.
- Bernfeld, P. (1955). *Methods in enzymology* (1st ed.). New York: Academic Press.
- Boni, F. I., Prezotti, F. G., & Cury, B. S. F. (2016). Gellan gum microspheres crosslinked with trivalent ion: Effect of polymer and crosslinker concentrations on drug release and mucoadhesive properties. *Drug Development and Industrial Pharmacy*, 29, 1–8.
- Bruschi, M. L., Jones, D. S., Panzeri, H., Gremião, M. P. D., Freitas, O., & Lara, E. H. G. (2007). Semisolid systems containing propolis for the treatment of periodontal disease: *In vitro* release kinetics, syringeability, rheological, textural, and mucoadhesive properties. *Journal of Pharmaceutical Sciences*, 96, 2074–2088.
- Caccavo, D., Lamberti, G., Cascone, S., Barba, A. A., & Larsson, A. (2015). Understanding the adhesion phenomena in carbohydrate-hydrogel-based systems: Water up-take, swelling and elastic detachment. *Carbohydrate Polymers*, 131, 41–49.
- Carvalho, F. C., Chorilli, M., & Gremião, M. P. D. (2014). Plataformas bio (muco) adesivas poliméricas baseadas em nanotecnologia para liberação controlada de fármacos-propriedades metodologias e aplicações. *Polímeros*, 24, 203–214.
- Chan, S., Chung, Y., Cheah, X., Tan, E. Y., & Quah, J. (2015). The characterization and dissolution performances of spray dried solid dispersion of ketoprofen in hydrophilic carriers. *Asian Journal of Pharmaceutical Sciences*, 10, 372–385.
- Cury, B. S. F., Castro, A. D., Klein, S. I., & Evangelista, R. C. (2009). Modeling a system of phosphated cross-linked high amylose for controlled drug release. Part 2: Physical parameters, cross-linking degrees and drug delivery relationships. *International Journal of Pharmaceutics*, 371, 8–15.
- Drechsler, M., Garbacz, G., Thomann, R., & Schubert, R. (2014). Development and evaluation of chitosan and chitosan/Kollicoat Smartseal 30 D film-coated tablets for colon targeting. *European Journal of Pharmaceutics and Biopharmaceutics*, 88, 807–815.
- Eouani, C., Piccerelle, P., Prinderre, P., Bourret, E., & Joachim, J. (2001). In-vitro comparative study of buccal mucoadhesive performance of different polymeric films. *European Journal of Pharmaceutics and Biopharmaceutics*, 52, 45–55.
- Felton, L. A. (2007). Characterization of coating systems. *AAPS PharmSciTech*, 8, 1–9.
- Fong, S. Y. K., Ibisogly, A., & Bauer-Brandt, A. (2015). Solubility enhancement of BCS class II drug by solid phospholipid dispersions: Spray drying versus freeze-drying. *International Journal of Pharmaceutics*, 496, 382–391.
- Fonseca, W. T., Santos, R. F., Alves, J. N., Ribeiro, S. D., Takeuchi, R. M., Santos, A. L., et al. (2015). Square wave voltammetry as analytical tool for real-time study of controlled naproxen release from cellulose derivative materials. *Electroanalysis*, 27, 1847–1854.
- Freire, C., Podczek, F., Veiga, F., & Sousa, J. (2009). Starch-based coatings for colon-specific delivery. Part II: Physicochemical properties and *in vitro* drug release from high amylose maize starch films. *European Journal of Pharmaceutics and Biopharmaceutics*, 72, 587–594.
- Gue, E., Willart, J. F., Muschert, S., Danede, F., Delcourt, E., Descamps, M., et al. (2013). Accelerated ketoprofen release from polymeric matrices: Importance of the homogeneity/heterogeneity of excipient distribution. *International Journal of Pharmaceutics*, 457, 298–307.
- Heinämäki, J., Halenius, A., Paavo, M., Alakurtti, S., Pitkänen, P., Pirttimaa, M., et al. (2015). Suberin fatty acids isolated from outer birch bark improve moisture barrier properties of cellulose ether films intended for tablet coatings. *International Journal of Pharmaceutics*, 489, 91–99.
- Kajjari, P. B., Manjeshwar, L. S., & Aminabhavi, T. M. (2014). Novel blend microspheres of cellulose triacetate and bee wax for the controlled release of nateglinide. *Journal of Industrial and Engineering Chemistry*, 20, 397–404.
- Komatsu, D., Otoguro, H., & Ruvoilo Filho, A. C. (2014). Avaliação comparativa entre os nanocompósitos de argila motmorilonita/ldpe e com hexaniobato de potássio/ldpe: caracterização das propriedades mecânicas e de transporte. *Polímeros*, 24, 37–44.
- Löbenberg, R., & Amidon, G. L. (2000). Modern bioavailability, bioequivalence and biopharmaceutics classification system. New scientific approaches to international regulatory standards. *European Journal of Pharmaceutics and Biopharmaceutics*, 50, 3–12.
- Liakos, I. L., D'aulilia, F., Garzoni, A., Bonferoni, C., Scarpellini, A., Brunetti, V., et al. (2016). All natural cellulose acetate–Lemongrass essential oil antimicrobial nanocapsules. *International Journal of Pharmaceutics* (in press).
- Lopes, C. M., Bettencourt, C., Rossi, A., Buttini, F., & Barata, P. (2016). Overview on gastroretentive drug delivery systems for improving drug bioavailability. *International Journal of Pharmaceutics*, 510, 144–158.
- Maestrelli, F., Zerrouk, N., Cirri, M., Mennini, N., & Mura, P. (2008). Microspheres for colonic delivery of ketoprofen-hydroxypropyl-cyclodextrin complex. *European Journal of Pharmaceutics and Biopharmaceutics*, 34, 1–11.
- Maestrelli, F., Zerrouk, N., Cirri, M., & Mura, P. (2015). Comparative evaluation of polymeric and waxy microspheres for combined colon delivery of ascorbic acid and ketoprofen. *International Journal of Pharmaceutics*, 485, 365–373.
- Maroni, A., Del Curto, M. D., Zema, L., Foppoli, A., & Gazzaniga, A. (2013). Film coatings for oral colon delivery. *International Journal of Pharmaceutics*, 457, 372–394.
- Meka, V. S., Dharmanlingam, S. R., & Kolapalli, V. R. M. (2014). Formulation of gastroretentive floating drug delivery system using hydrophilic polymers and its *in vitro* characterization. *Brazilian Journal of Pharmaceutical Sciences*, 50, 431–439.
- Meneguín, A. B., Cury, B. S. F., & Evangelista, R. C. (2014). Films from resistant starch-pectin dispersions intended for colonic drug delivery. *Carbohydrate Polymers*, 99, 140–149.
- Milovanovic, S., Markovic, D., Aksentijevic, K., Stojanovic, D. B., Ivanovic, J., & Zizovic, I. (2016). Application of cellulose acetate for controlled release of thymol. *Carbohydrate Polymers*, 147, 344–353.
- Mizoguchi, M., Nakatsuji, M., Inoue, H., Yamaguchi, K., Sakamoto, A., Wada, K., et al. (2015). Novel oral formulation approach for poorly water-soluble drug using lipocalin-type prostaglandin D synthase. *European Journal of Pharmaceutical Sciences*, 74, 77–85.
- Moustafine, R. I., Zaharov, I. M., & Kemenova, V. A. (2006). Physicochemical characterization and drug release properties of Eudragit EP/Eudragit L 100-55 interpolyelectrolyte complexes. *European Journal of Pharmaceutics and Biopharmaceutics*, 63, 26–36.
- Mu, H., Holm, R., & Müllertz, A. (2013). Lipid-based formulations for oral administration of poorly water-soluble drugs. *International Journal of Pharmaceutics*, 453, 215–224.
- Mundargi, R. C., Patil, S. A., & Aminabhavi, T. M. (2007). Evaluation of acrylamide-grafted-xanthan gum copolymer matrix tablets for oral controlled delivery of antihypertensive drugs. *Carbohydrate Polymers*, 69, 130–141.
- Mwesigwa, E., & Basit, A. W. (2016). An investigation into moisture barrier film coating efficacy and its relevance to drug stability in solid dosage forms. *International Journal of Pharmaceutics*, 497, 70–77.
- Nep, E. I., Asare-Addo, K., Ghorri, M. U., Conway, B. R., & Smith, A. M. (2015). Starch-free gawia gum matrices: Compaction, swelling, erosion and drug release behavior. *International Journal of Pharmaceutics*, 496, 689–698.
- Papadopoulou, V., Kosmidis, K., Vlachou, M., & Macheras, P. (2006). On the use of the Weibull function for the discernment of drug release mechanisms. *International Journal of Pharmaceutics*, 309, 44–50.
- Perontis, S., Hatzidimitriou, A. G., Begou, O., Papadopoulou, A. N., & Psomas, G. (2016). Characterization and biological properties of copper(II)-ketoprofen complexes. *Journal of Inorganic Biochemistry*, 162, 22–30.
- Prezotti, F. G., Cury, B. S. F., & Evangelista, R. C. (2014). Mucoadhesive beads of gellan gum/pectin intended to controlled delivery of drugs. *Carbohydrate Polymers*, 113, 286–295.
- Prezotti, F. G., Meneguín, A. B., Evangelista, R. C., & Cury, B. S. F. (2012). Preparation and characterization of free films of high amylose/pectin mixtures crosslinked with sodium trimetaphosphate. *Drug Development and Industrial Pharmacy*, 38, 1–6.
- Rodrigues Filho, G., Almeida, F., Ribeiro, S. D., Tormin, T. F., Muñoz, R. A. A., Assunção, R. M. N., et al. (2015). Controlled release of drugs from cellulose acetate matrices produced from sugarcane bagasse: Monitoring by square-wave voltammetry. *Drug Development and Industrial Pharmacy*, 23, 1–7.
- Rodrigues Filho, G., Ribeiro, S. D., Meireles, C. S., Silva, L. G., Ruggiero, R., Ferreira Junior, M. F., et al. (2011). Release of doxycycline through cellulose acetate symmetric and asymmetric membranes produced from recycled agroindustrial residue: Sugarcane bagasse. *Industrial Crops and Products*, 33, 566–571.
- Ruggiero, R., Carvalho, V. A., Silva, L. G., Magalhães, D., Ferreira, J. A., Menezes, H. H. M., et al. (2015). Study of *in vitro* degradation of cellulose acetate membranes modified and incorporated with tetracycline for use as an adjuvant in periodontal reconstitution. *Industrial Crops and Products*, 72, 2–6.
- Shende, P. K., Gaud, R. S., Bakal, R., & Patil, D. (2015). Effect of inclusion complexation of meloxicam with  $\beta$ -cyclodextrin- and  $\beta$ -cyclodextrin-based nanosponges on solubility, *in vitro* release and stability studies. *Colloids and Surfaces B: Biointerfaces*, 136, 105–110.
- Smart, J. (2005). The basics and underlying mechanisms of mucoadhesion. *Advanced Drug Delivery Reviews*, 57, 1556–1568.
- Sosnik, A., Neves, J., & Sarmento, B. (2014). Mucoadhesive polymers in the design of nano-drug delivery systems for administration by non-parenteral routes: A review. *Progress in Polymer Science*, 39, 2030–2075.
- Varum, F. J. O., Hatton, G. B., & Basit, A. W. (2013). Food, physiology and drug delivery. *International Journal of Pharmaceutics*, 457, 446–460.
- Wang, Y., Han, X., Wang, J., & Wang, Y. (2016). Preparation, characterization and *in vivo* evaluation of amorphous tacrolimus nanosuspensions produced using CO<sub>2</sub>-assisted *in situ* nanoamorphization method. *International Journal of Pharmaceutics*, 505, 35–41.
- Włodarski, K., Sawicki, W., Haber, K., Knapik, J., Wojnarowska, Z., Paluch, M., et al. (2015). Physicochemical properties of tadalafil solid dispersions—Impact of polymer on the apparent solubility and dissolution rate of tadalafil. *European Journal of Pharmaceutics and Biopharmaceutics*, 94, 106–115.

- Xia, D., Quan, P., Piao, H., Piao, H., Sun, S., Yin, Y., et al. (2010). Preparation of stable nitrendipine nanosuspensions using the precipitation–ultrasonication method for enhancement of dissolution and oral bioavailability. *European Journal of Pharmaceutics and Biopharmaceutics*, 40, 325–334.
- Yu, D. G., Li, X. Y., Wang, X., Chian, W., Liao, Y. Z., & Li, Y. (2013). Zero-order drug release cellulose acetate nanofibers prepared using coaxial electrospinning. *Cellulose*, 20, 379–389.
- Yu, D. G., Yang, C., Jin, M., Williams, G. R., Zou, H., Wang, X., et al. (2016). Medicated Janus fibers fabricated using a Teflon-coated side-by-side spinneret. *Colloids and Surfaces B: Biointerfaces*, 138, 110–116.
- Zhang, Y., Chan, J. W., Moretti, A., & Uhrich, K. E. (2015). Designing polymers with sugar-based advantages for bioactive delivery applications. *Journal of Controlled Release*, 219, 355–368.